Novel Pattern Recognition Method for Analysis the Radiation Exposure in Cancer Treatment

Dmitriy Dubovitskiy(✉) and Valeri Kouznetsov

Oxford Recognition Ltd, 10 Maio Road, Cambridge CB4 2GA, UK
{dda,vk}@oxreco.com
http://www.oxreco.com

Abstract. A novel pattern recognition technique has been deployed in the treatment of cancer tumours to provide improved targeting of ionising radiation and more accurate measurement of the radiation dose. The radiation beams enter the body from different directions to concentrate on the tumour. The centre of the tumour has to be precisely located relatively to patient's skin surface, so the radiation does not affect healthy tissue and produces successful treatment. Existing methods of 3D dose measurement are highly labor-intensive and generally suffer from low accuracy. In this publication, we propose a new method of 3D measurement of the dose in real-time by using skin pattern recognition technology. The textural pattern of the patient's skin is analysed from an image sensor in a specially designed camera using Fractal Geometry and Fuzzy logic. A specially designed net sensor is then placed over the area of skin exposed to the treatment in order to measure the radiation dose. The algorithms discussed below enable the precise focussing of the radiation. The novel object recognition technique provides a mathematical tool to build a volume model of the dose distribution inside the patient's body. This paper provides an overview and specific information on the technology and necessary background for future industrial implementation into health care infrastructure.

Keywords: Cancer treatment · In vivo dosimetry
Radiation sensors · Pattern analysis · Decision making
Object recognition · Image morphology · Image recognition
Pattern recognition · Texture classification · Computational geometry

1 Introduction

For the purposes of the dosimetry of the small areas in radiotherapy, typically uses traditional micro ionisation chambers, semiconductor diode dosimeters and, in the recent years, increasingly uses a very handy MOSFET transistors. The MOSFET transistors provide good accuracy and repeatability of the results with dimensions of a few millimetres, which is sufficient for practical applications in

N. Peixoto et al. (Eds.): BIOSTEC 2017, CCIS 881, pp. 106–118, 2018.
https://doi.org/10.1007/978-3-319-94806-5_6

medical diagnostics. In addition, they are joined harmoniously with the systems of scanning and information processing [1,2]. For 3D doisimetry, Gel Dosimeters proposed in the mid 80-s are widely used. However, this method is rather inconvenient as it is associated with the use of special phantoms (models) made of gel-like material changing its optical properties under the influence of ionising irradiation. At the same time, it allows customising the parameters intensity and the 3D geometry of irradiation. Polymer gel dosimetry remains one of the most promising and widely used tools for 3D dose measuring [3]. There are also methods of extrapolating measurements at individual points or 2D measurements to 3D models.

The most modern methods [4] of measurement suggest usage of linear array diodes with 98 measurement points for scanning of a water phantom. Then the data are linked to the patient CT image and after Monte Carlo method are used to extrapolate dose distributions inside the patient body and to control measurements with point dosimeters (diodes) performed during the process treatment in vivo. Impact of ionising irradiation at different MOS (metal oxide semiconductor) structures have been studied for quite a long time, at least since the mid 70-s due to the start of using of electronics based on MOS technology in space systems [5]. The processes occurring in such structures under the influence of radiation of various types and intensity is very well studied and described in numerous articles addressing radiation hardness of MOS IS [6–9]. For medical applications measuring of the accumulated radiation dose with such structures is still rather new. As an indication of the accumulated dose the effect of degradation of MOS structure is used, particularly the under-gate dielectric (SiO2). Without going deep into the details of physical processes, we mention only the main effect that is used for dosimetry.

Under irradiation, gate dielectric accumulates a positive charge which leads in particular to a shift of the threshold voltage in a MOSFET transistor or to a shift of the volt-farad characteristics of the MOS capacitor. Inducing of a positive voltage on the Gate of a transistor (MOS capacitor) in the process of irradiation, leads to the increase of the amount of accumulated charge. In the case of no voltage applied, it makes possible to irradiate the passive MOS structure, and then to measure the charge that is equivalent to the dose. Other effects occurring in dielectrics during irradiation can be ignored in this case. In the range of doses used in medicine, the charge accumulation is linearly proportional to the dose and only at high doses about 6–8 Gy (depends on the technology) tends to saturation and loses linearity. Moreover, dosimeters based on MOS structures are small in size (around 1 sq. mm) and very simple in production.

The particular focus of this paper is in the use of such sensors for development and imaging technology of a net bandage dosimetry system (Fig. 1), with a MOS capacitor sensor in every node of the grid. Such dosimetry net can be placed (dressed) around any part of the body (or fantom) and will allow controlling the dose of radiation for the incoming and outgoing flow of irradiation and from any direction. This will allow building a 3D model of the absorbed dose inside the

patient's body, which is a new and highly demanded product in the market of medical diagnostics tools.

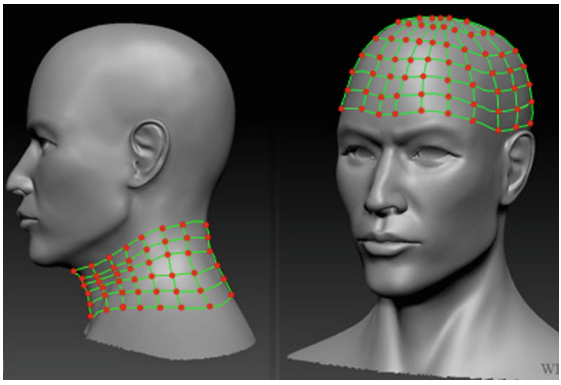

Fig. 1. Net bandage.

The skin pattern recognition system is to deliver the location for net bandage position relatively to body map. The skin patent is mathematically interpreted by Fractal geometry. The self-similarity features of fractals are very suitable for this application. The skin region is translated into the vector of Fractal features. The Fractal features is then identifying the skin map. The first net bandage placement is to select and record the skin regions. The future treatments requires to position the sensor net at the very same skin area.

The automatic decision making system is implemented by Fuzzy logic technology. At the first net sensor bandage application the image recognition system build membership function of Fuzzy logic and memorised skin map. The future net bandage application will be automatically calculated offset to the first position and it is up to future developer to use the offset or to move the sensors net to the exact first position. We will cover the novel mathematical equation in Sect. 3 and begin from dosimetry setup in next section.

2 Structural Scheme of Dosimetry System

The proposed dosimetric network, can be a convenient and inexpensive tool to verify the dose distribution inside the body as well as build three-dimensional models of absorbed dose. The MOSFET was recently highly proven [10–14] as an in vivo dosimeter of the absorbed dose. Here, we have decided to focus on the most simple structures, such as the MOS capacitors, since the phenomenon of charge accumulation in under-gate dielectric of MOSFET (in fact, under-gate MOS capacitor) determines its ability to function as a dosimeter. MOS sensors, in this case, contain a number of advantages. MOS capacitors are extremely simple and inexpensive to manufacture. We can select and vary many parameters of

this structure (for example thickness and type of gate-dielectric, the size of the structure) to improve its operation as a dosimeter, due to the fact it's simply a capacitor it is not necessary to take into consideration the parameters required for function as a transistor.

The scheme of the measurement of accumulated charge which corresponds to the absorbed dose requires less number of contacts (only two, and one of them is common for all sensors) that facilitates the creation of matrix or grid with a large number of sensors.

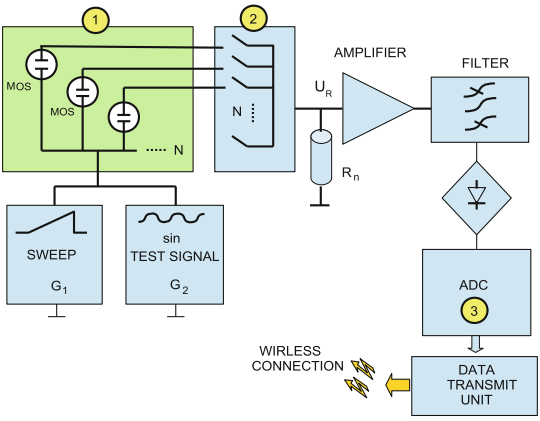

Fig. 2. The measuring system for collecting data from sensors. 1- matrix of sensors, 2-multiplexer, 3-analog to digital converter.

The block diagram of such a system as shown in Fig. 2. The accumulated charge in the oxide (equivalent to dose) proposed to determine by measuring volt-farad characteristics. This method has long been known as the main and classical method for measurement of MOS structures properties [15–17] and have been well tested. A typical view of this characteristic for the silicon substrate n-type is shown in the Fig. 3.

This figure shows the shift of C-V characteristics which occurs as a result of accumulating charge in the gate oxide, the measurement of this shift is our goal in this case. Capacitive Sensors - dosimeters are connected in matrix (1). The date from the sensors is collected consecutively been analog multiplexer (2) switches from one structure to another. The sweep generator G1 provides a slow shift in a range of a few volts on MOS and G2 provides a test signal with a frequency of 1 MHz and amplitude of 10 mV. The alternate voltage amplitude on resistor Rn will be proportional to the capacity of MOS sensor, as demonstrated in the formulas below.

$$Rc = 1/wC, \quad i = Ug_2/Z = Ug_2/\sqrt{Rn^2 + 1/w^2C^2}$$

$$if \quad R_c = 1/wC >> R_n, \quad then \quad i \approx wC(Ug_1)Ug_2$$

$$U_R = iR_n = Ug_2R_nwC(Ug_1) \quad where \quad w = 2\pi f$$

The measurement process for each sensor will take approximately no more than 5–10 ms. This means that the matrix of sensors with dimension of 256 sensors will be scanned in 1.5 to 2.5 s. These data is digitised by ADC (3) and sent to a computer wirelessly, where data can be processed further. The advantages of MOS as an absorbed dose dosimeters is also that they are able keep the charge somewhat stable and readings can be taken for a long period of time after exposure.

When MOS capacitors are exposed to ionizing radiation, the positive charge is captured in the under-gate oxide [18–20]. It leads to a shift of volt-farad characteristics, see Fig. 3. The magnitude of the shift depends on the absorbed dose of ionising radiation and is approximately 200 mV in the absence of gate voltage during irradiation. By applying a positive voltage on the gate, we can increase the sensitivity of the sensors and the shift of the voltage can reach 400–500 mV per Gy.

To confirm the behaviour of MOS structures under radiation by standard medical equipment, the most common samples taken, the gate oxide SiO2 were grown in a dry environment at 1000C, thickness of oxide was 0.6 µm on Si wafer 4.5 Om/cm conductivity of n-type with F(fluorine) doping. Size of crystal was 1×1 mm. Irradiation was carried out at Photon clinical linear accelerator 6 MeV (Varian 2100 EX), doses were 0 to 10 Gy, at room temperature. As a control dosimeter, ionisation chamber ROOS was used. Results of the experiment are shown on Fig. 4.

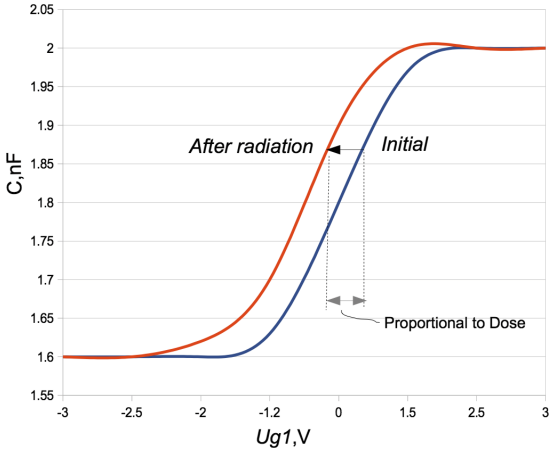

Fig. 3. Volt-Farad characteristic of typical MOS condensator.

For our purposes we are going to use a successfully tested system of pattern recognition [27] and adhere our system of sensors to the skin of the patient. The image recognition system was used for skin cancer diagnostic and has been published in [22–26,28] this redundant system was working well and we expect it to be extremely effective.

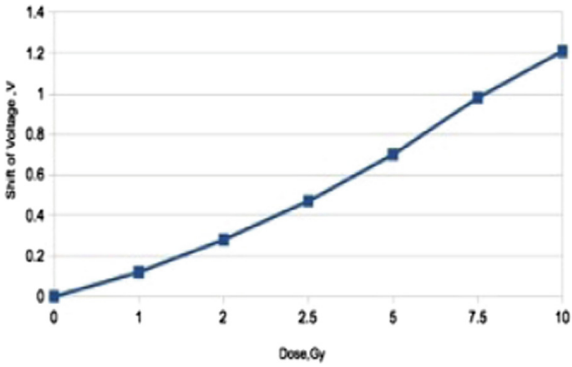

Fig. 4. Characteristic of volt shift for the silicon substrate n-typer.

3 Skin Pattern Positioning System

The current medical practice includes several radiation exposure during the course of treatment with a number of days in between. The position of the net bandage on the patient's skin is very important to allow consistency for the next treatment of the same tumour. In order to address this, data from the CT scan could be used to adjust position for the next treatment. Computation of position is implemented by using Fractal Geometry theory [36] to get the precise pattern of the skin. The precise pattern of the skin is corresponded to the calibration points on the net bandage. The real time computation system [33] will allow a doctor to dynamically move the bandage and see the offset from the last treatment position. When offset approaches zero, the exact same position of the radiation sensors will be reached.

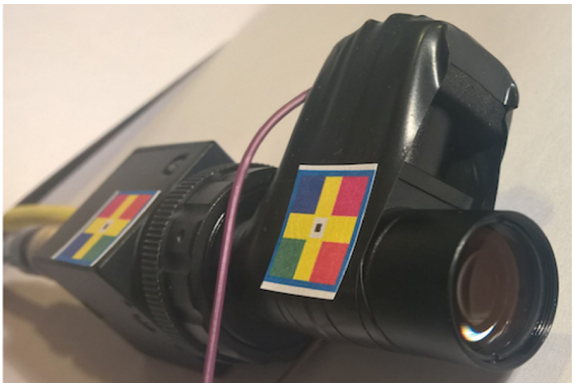

Fig. 5. Dermatological image acquisition camera.

The skin has texture and a particular skin region can be characterised by Fractal features called Fractal parameters [34]. An image of the skin sample is taken by a specially designed dermatological image acquisition camera [38] on Fig. 5.

The correspondent points are calculated from Fractal parameters [35]. If we consider the profile of a typical skin image [37], then the curve does not coincide with a sine-wave signal. To obtain adequate accuracy, it is necessary to magnify the resolution of the image [21], which in turn introduces distortion [29,31]. For increased accuracy on low-resolution data, we consider a convolution function of a form more consistent with the profile of a video signal [30–32]. For a signal I we consider the representation

$$F(k) = \sum_{n=1}^{N} I(n)$$

$$\arccos\left[\cos\left(\frac{2\pi(\mathrm{k}-1)(\mathrm{n}-1)}{N} - \frac{\pi}{2}\right)\right] - \frac{\pi}{2}$$

$$-i \arcsin\left[\cos\left(\frac{2\pi(\mathrm{k}-1)(\mathrm{n}-1)}{N}\right)\right]$$

and for an image I with resolution $m \times n$,

$$F(p,q) = \sum_{m=1}^{M}\sum_{n=1}^{N} I(m,n) \tag{1}$$

$$\left(\arccos\left[\cos\left(\frac{2\pi(p-1)(m-1)}{M} - \frac{\pi}{2}\right)\right] - \frac{\pi}{2}\right)$$

$$\times \left(\arccos\left[\cos\left(\frac{2\pi(k-1)(n-1)}{N} - \frac{\pi}{2}\right)\right] - \frac{\pi}{2}\right)$$

$$- i \arcsin\left[\arccos\left(\frac{2\pi(k-1)(p-1)}{M}\right)\right]$$

$$\times \arcsin\left[\cos\left(\frac{2\pi(k-1)(n-1)}{N}\right)\right] \tag{2}$$

In this work, application of the power spectrum method used to compute the fractal dimensions of a skin surface is based on the above representations for $F(k)$ and $F(p,q)$ respectively. We then consider the power spectrum of an ideal fractal signal given by $P = c|k|^{-\beta}$, where c is a constant and β is the spectral exponent. In two dimensions, the power spectrum is given by $P(k_x, k_y) = c|k|^{-\beta}$, where $|k| = \sqrt{k_x^2 + k_y^2}$. In both cases, application of the least squares method or Orthogonal Linear Regression yields a solution for β and c, the relationship between β and the Fractal Dimension D_F being given by

$$D_F = \frac{3D_T + 2 - \beta}{2}$$

for Topological Dimension D_T. This approach allows us to drop the limits on the recognition of small objects since application of the FFT (for computing the

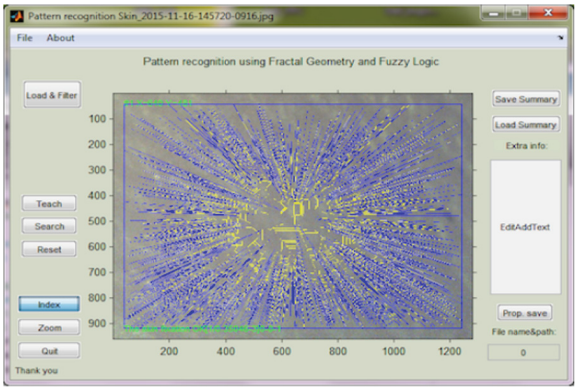

Fig. 6. GUI software.

power spectrum) works well (in terms of computational accuracy) only for large data sets, i.e. array sizes larger than 256 and 256×256. Tests on the accuracy associated with computing the fractal dimension using Eqs. (1) and (2) show an improvement of 5% over computations based on conventional Discrete Fourier Transform.

The setup calculates Fractal features dynamically from the centre of an image. The testing GUI software is presented on Fig. 6:

The original skin image from the camera is presented on Fig. 7.

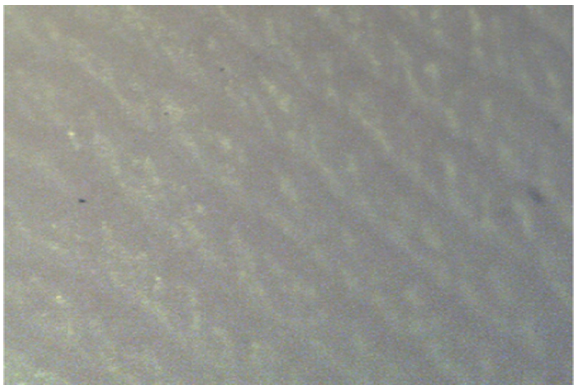

Fig. 7. The original skin image.

The current position of the net bandage and camera is given from optical calibration marks Fig. 8.

The corresponding points of the current Fractal marks and optical position gives us the offset number which guide the doctor to the original position of the sensor net bandage.

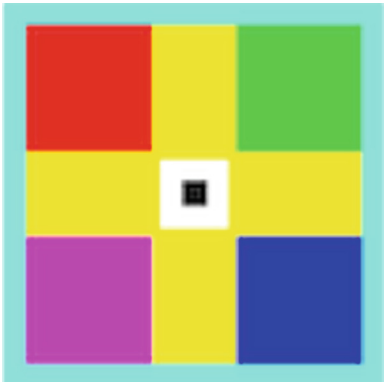

Fig. 8. The optical calibration mark.

In order to map the skin surface, the 'system' has to know its mathematical representation. Here, this representation is based on the features considered in the previous section which are used to create an image of the object in the 'electronic mind'. This includes the textural features for the skin object coupled with the Euclidean and morphological measures defined. In the case of a general application, all objects are represented by a list of parameters for implementation of supervised learning for the first net bandage application in which a fuzzy logic system automatically adjusts the weight coefficients for the input feature set.

The methods developed represent a contribution to pattern recognition based on fractal geometry, fuzzy logic and the implementation of a fully automatic recognition scheme as illustrated in Fig. 9 for the Fractal Dimension D (just one element of the feature vector used in practice). The recognition procedure

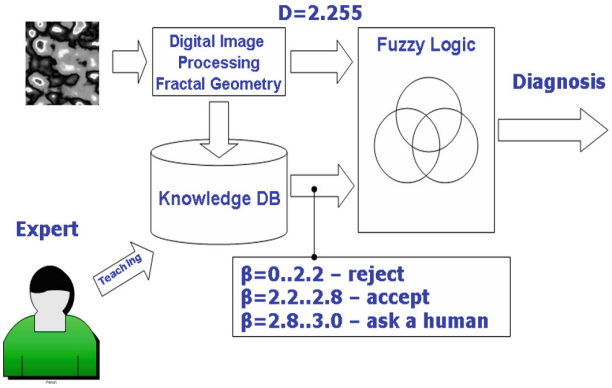

Fig. 9. Basic architecture of the diagnostic system based on the Fractal Dimension D (a single feature) and decision making criteria β.

uses the decision making rules from fuzzy logic theory [39–42] based on all, or a selection, of the features defined above which are combined to produce a feature vector $\mathbf{x}$.

3.1 Decision Making

The class probability vector $\mathbf{p} = \{p_j\}$ is estimated from the object feature vector $\mathbf{x} = \{x_i\}$ and membership functions $m_j(\mathbf{x})$ defined in a knowledge database. If $m_j(\mathbf{x})$ is a membership function, then the probability for each j^{th} class and i^{th} feature is given by

$$p_j(\mathbf{x}_i) = \max\left[\frac{\sigma_j}{|\mathbf{x}_i - \mathbf{x}_{j,i}|} \cdot m_j(\mathbf{x}_{j,i})\right]$$

where σ_j is the distribution density of values $\mathbf{x}_j$ at the point $\mathbf{x}_i$ of the membership function. The next step is to compute the mean class probability given by

$$\langle p \rangle = \frac{1}{j} \sum_j \mathbf{w}_j p_j$$

where $\mathbf{w}_j$ is the weight coefficient matrix. This value is used to select the class associated with

$$p(j) = \min\left[(p_j \cdot \mathbf{w}_j - \langle p \rangle) \geq 0\right]$$

providing a result for a decision associated with the j^{th} class. The weight coefficient matrix is adjusted during the learning stage of the algorithm.

The decision criterion method considered here represents a weighing-density minimax expression. The estimation of the decision accuracy is achieved by using the density function

$$d_i = |\mathbf{x}_{\sigma_{\max}} - \mathbf{x}_i|^3 + [\sigma_{\max}(\mathbf{x}_{\sigma_{\max}}) - p_j(\mathbf{x}_i)]^3$$

with an accuracy determined by

$$P = \mathbf{w}_j p_j - \mathbf{w}_j p_j \frac{2}{\pi} \sum_{i=1}^{N} d_i.$$

3.2 Skin Pattern Learning

The Pattern learning procedure is the most important part of the system for operation in automatic recognition mode. The training set of sample objects should cover all ranges of class characteristics with a uniform distribution together with a universal membership function. This rule should be taken into account for all classes participating in the training of the system. An system defines the class and accuracy for each model object where the accuracy is the level of self confidence that the skin object belongs to a given class. During this procedure, the system computes and transfers to a knowledge database, a vector

$\mathbf{x} = \{x_i\}$, which forms the membership function $m_j(\mathbf{x})$. The matrix of weight factors $w_{j,i}$ is formed at this stage accordingly for the i^{th} parameter and j^{th} class using the following expression:

$$w_{i,j} = \left| 1 - \sum_{k=1}^{N} \left(p_{i,j}(\mathbf{x}_{i,j}^k) - \langle p_{i,j}(\mathbf{x}_{i,j}) \rangle \right) p_{i,j}(\mathbf{x}_{i,j}^k) \right|.$$

The result of the weight matching procedure is that all parameters which have been computed but have not made any contribution to the characteristic set of an object are removed from the decision making algorithm by setting $w_{j,i}$ to null.

4 Conclusions

The focus of this paper is the development and validation of a simple, user-friendly system which allows control of the spatial distribution of the accumulated dose of radiation inside a body. The use of modern image recognition techniques allows precise positioning of the sensors net bandage. The calculation of exact accumulation dose and its confirmation by correct measurements is the key to the effective treatment. Simple and reliable monitoring of the 3D dose distribution will allow us to provide treatment in the safest way. The safe way means that the healthy cells will not be subject to unnecessary exposure, which helps to maintain the healthy cells surrounding the tumour. This work represents a new approach to accurate radiation exposure treatments. Implementation in hospitals requires more experiments, calibration and technological input. Feasibility studies, clinical validation and economical evaluation should be the next steps. We hope that this research will contribute to the safer radiation exposure treatment in cancer cure and prolonging the lives of many people.

Acknowledgement. The work reported in this paper is supported by the Oxford Recognition Ltd. The authors are grateful to Richard Spooner, Ann Wallace and Gladys O'Brien for help in the preparation of this paper.

References

1. Soubra, M., Cygler, J., Mackay, G.F.: Evaluation of a dual metal oxide-silicon semiconductor field effect transistor detector as a radiation dosimeter. Med. Phys. **21**(4), 567–572 (1984)
2. Thomson I., Reece M.H.: Semiconductor MOSFET dosimetry. In: Proceedings of Health Physics Society Annual Meeting (1988)
3. De Deene, Y., Jirasek, A.: Uncertainty in 3D gel dosimetry. J. Phys. Conf. Series **573**, 012008 (2015). 8th International Conference on 3D Radiation Dosimetry (IC3DDose)
4. Nithiyanantham, K., Mani, G.K., Subramani, V., Mueller, L., Palaniappan, K.K., Kataria, T.: Analysis of direct clinical consequences of MLC positional errors in volumetric-modulated arc therapy using 3D dosimetry system. J. Appl. Clin. Med. Phys. **16**(5), 296–305 (2015)

5. Ma, T.P., Dressendorfer, P.V.: Ionizing Radiation Effects in MOS Devices and Circuits. Wiley Interscience, New York (1989)
6. Kohler, R.A., Kushner, R.A.: Total dose radiation hardness of MOS devices in hermetic ceramic packages. IEEE Trans. Nucl. Sci. **35**(6), 1492–1496 (1988)
7. Kaschieva, S.: Improving the radiation hardness of MOS structures. Int. J. Electron. **76**(5), 883–886 (1994)
8. Claeys, C.: Simoen, E: Radiation Effects in Advanced Semiconductor Materials and Devices. Springer Science and Business Media, Berlin (2002). https://doi.org/10.1007/978-3-662-04974-7
9. Meurant, G.: New Insulators Devices and Radiation Effects, 1st edn. North Holland, New York (1999). Print book ISBN 9780444818010
10. Kumar, A.S., Sharma, S.D., Paul Ravindran, B.: Characteristics of mobile MOSFET dosimetry system for megavoltage photon beams. J. Med. Phys. **39**(3), 142–149 (2014)
11. Gopidaj, A., Billimagga, R.S., Ramasubramanian, V.: Performance characteristics and commissioning of MOSFET as an in-vivo dosimeter for high energy photon external beam radiation therapy. Rep. Pract. Oncol. Radiother. **13**(3), 114–125 (2008)
12. Choe, B.-Y.: Dosimetric characteristics of standard and micro MOSFET dosimeters as in-vivo dosimeter for clinical electron beam. J. Korean Phys. Soc. **55**, 2566–2570 (2013)
13. Briere, T.M., et al.: In vivo dosimetry using disposable MOSFET dosimeters for total body irradiation. Med. Phys. **32**, 1996 (2005)
14. Scalchi, P., Francescon, P., Rajaguru, P.: Characterisation of a new MOSFET detector configuration for in vivo skin dosimetry. Med. Phys. **32**(6), 1571–1578 (2005)
15. Sze, S.M.: Physics of Semiconductor Devices, 2nd edn. Willey, New York (1981)
16. Nicollian, E.H., Brews, J.R.: MOS (Metal Oxide Semiconductor) Physics and Technology. Wiley, New York (1982)
17. Zemel, J.N.: Nondestructive Evaluation of Semiconductor Materials and Devices. Nato Science Series B. Springer US, New York (1979). ISSN 0258-1221
18. Hughes, H.L., Benedetto, J.M.: Radiation effects and hardening of MOS technology devices and circuits. IEEE Trans. Nucl. Sci. **50**, 500–521 (2003)
19. Oldham, T.R., McLean, F.B.: Total ionizing dose effects in MOS oxides and devices. IEEE Trans. Nucl. Sci. **50**, 483–499 (2003)
20. Adams, J.R., Daves, W.R., Sanders, T.J.: A radiation hardened field oxide. IEEE Trans. Nucl. Sci. **NS–24**(6), 2099–2101 (1977)
21. Davies, E.R.: Machine Vision: Theory, Algorithms, Practicalities. Academic press, London (1997)
22. Dubovitskiy, D.A., Blackledge, J.M.: Surface inspection using a computer vision system that includes fractal analysis. ISAST Trans. Electron. Signal Process. **2**(3), 76–89 (2008)
23. Dubovitskiy, D.A., Blackledge, J.M.: Texture classification using fractal geometry for the diagnosis of skin cancers. In: EG UK Theory and Practice of Computer Graphics 2009, pp. 41–48 (2009)
24. Dubovitskiy, D., Devyatkov, V., Richer, G.: The application of mobile devices for the recognition of malignant melanoma. In: BIODEVICES 2014: Proceedings of the International Conference on Biomedical Electronics and Devices, Angers, France, p. 140, 03–06 March 2014. ISBN 978-989-758-013-0

25. Dubovitskiy, D.A., Blackledge, J.M.: Moletest: a web-based skin cancer screening system. In: The Third International Conference on Resource Intensive Applications and Services, Venice, Italy, vol. 978-1-61208-006-2, pp. 22–29, 22–27 May 2011
26. Dubovitskiy, D.A., Blackledge, J.M.: Object Detection and classification with applications to skin cancer screening. In: International Society for Advanced Science and Technology (ISAST) Intelligent Systems, vol. 1, no. 1, pp. 34–45 (2008). ISSN 1797–1802
27. Dubovitskiy, D.A., Blackledge, J.M.: Targeting cell nuclei for the automation of raman spectroscopy in cytology. In: Targeting Cell Nuclei for the Automation of Raman Spectroscopy in Cytology. British Patent No. GB1217633.5 (2012)
28. Dubovitskiy, D.A., McBride, J.: New 'spider' convex hull algorithm for an unknown polygon in object recognition. In: BIODEVICES 2013: Proceedings of the International Conference on Biomedical Electronics and Devices, p. 311 (2013)
29. Freeman, H.: Machine Vision: Algorithms, Architectures, and Systems. Academic press, London (1988)
30. Grimson, W.E.L.: Object Recognition by Computers: The Role of Geometric Constraints. MIT Press, Cambridge (1990)
31. Louis, J., Galbiati, J.: Machine Vision and Digital Image Processing Fundamentals. State University of New York, New-York (1990)
32. Nalwa, V.S., Binford, T.O.: On detecting edge. IEEE Trans. Pattern Anal. Mach. Intell. **1**(PAMI–8), 699–714 (1986)
33. Ripley, B.D.: Pattern Recognition and Neural Networks. Academic Press, Oxford (1996)
34. Clarke, K., Schweizer, D.: Measuring the fractal dimension of natural surfaces using a robust fractal estimator. Cartograph. Geograph. Inf. Syst. **18**, 27–47 (1991)
35. Falconer, K.: Fractal Geometry. Wiley, Hoboken (1990)
36. DeCola, L.: Fractal analysis of a classified landsat scene. Photogram. Eng. Remote Sens. **55**(5), 601–610 (1989)
37. Snyder, W.E., Qi, H.: Machine Vision. Cambridge University Press, Cambridge (2004)
38. Yagi, Y., Gilberson, J.R.: Digital imaging in pathology: the case for standardisation. J. Telemed. Telecare **11**, 109–116 (2005)
39. Zadeh, L.A.: Fuzzy Sets and Their Applications to Cognitive and Decision Processes. Academic Press, New York (1975)
40. Mamdani, E.H.: Advances in linguistic synthesis of fuzzy controllers. J. Man. Mach. **8**, 669–678 (1976)
41. Sanchez, E.: Resolution of composite fuzzy relation equations. Inf. Control **30**, 38–48 (1976)
42. Vadiee, N.: Fuzzy Rule Based Expert System-I. Prentice Hall, Englewood (1993)